ESD-TR-77-115

Technical Note

1977-18

R. Weber

Photoemissive and Electroemissive Surfaces and Sandwiches

25 May 1977

Prepared for the Department of the Air Force
under Electronic Systems Division Contract F19628-76-C-0002 by

Lincoln Laboratory

MASSACHUSETTS INSTITUTE OF TECHNOLOGY

LEXINGTON, MASSACHUSETTS

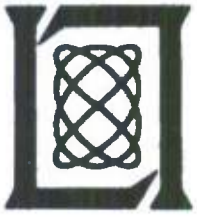

The work reported in this document was performed at Lincoln Laboratory, a center for research operated by Massachusetts Institute of Technology, with the support of the Department of the Air Force under Contract F19628-76-C-0002.

This technical report has been reviewed and is approved for publication.

FOR THE COMMANDER

Raymond L. Loiselle

Raymond L. Loiselle, Lt. Col., USAF
Chief, ESD Lincoln Laboratory Project Office

MASSACHUSETTS INSTITUTE OF TECHNOLOGY
LINCOLN LABORATORY

PHOTOEMISSIVE AND ELECTROEMISSIVE SURFACES AND SANDWICHES

R. WEBER
Group 94

TECHNICAL NOTE 1977-18

25 MAY 1977

LEXINGTON MASSACHUSETTS

ABSTRACT

Several commercially available photoemissive surfaces (PES) and electroemissive surfaces (ES) are evaluated to find: 1. the most efficient PES in the presence of sunlight-like optical signals, and, 2. the most efficient ES/PES combination ("sandwich") for the transition between stages in an optical sensor employing, for example, an image intensifier tube coupled to an ebsicon-type camera tube. In the first case, an S-20VR PES is shown to be superior; while in the second case, a P-11/S-20 sandwich is shown to be the superior combination.

PHOTOEMISSIVE AND ELECTROEMISSIVE SURFACES AND SANDWICHES

In an earlier Note,[1] flux rate density standards for sunlight incident on S-20 and S-25 photoemissive surfaces were developed. The present Note builds on that report to consider additional photoemissive surfaces, and is extended to consider the case in which a phosphor is the "source" for a photoemissive surface. The intent here is to specify an optimum first photosurface for an ebsicon-type tube and an optimum phosphor/photoemissive-surface combination ("sandwich") for the design of an externally intensified ebsicon-type camera tube. The optical signal of interest is assumed to have the spectral characteristics of sunlight. Only those materials which have been presented in the commercial literature as being available in large-area formats (40 mm to 80 mm) have been considered in this work.

Figure 1 presents the quantum efficiencies of five photoemissive surfaces and the "smoothed" photon flux rate density of sunlight through one standard air mass[1] as functions of the wavelength. The S-20 curve is the typical curve described earlier,[1] while the MA-2 and MA-4 curves are from ITT data, the S-20VR curve is from VARO data, and the 119/131 curve is from RCA data.

The photoelectron flux rate densities for sunlight over the wavelength range of 0.300 to 0.920 micron have been obtained by "multiplying" the spectral curve of each surface with the flux curve of sunlight in intervals of .020 micron. The results of these convolutions, normalized to the S-20/sun product, are shown in Table 1. The S-20VR/sunlight result is better than the standard S-20/sunlight result by a factor of 1.20, or $0^m.20$ detector magnitudes. This corresponds, approximately, to the "gain" of one air mass at an elevated ($\approx$1500 m) electro-optical site on a photometric night. In the detection of space objects by reflected sunlight, assuming the spectrum unchanged by reflection, this signal gain of $0^m.02$ is directly translatable to an increased detection capability of $0^m.10$ on a typical night. It is to be noted that if the spectrum should depart from that of sunlight under reflection, then the

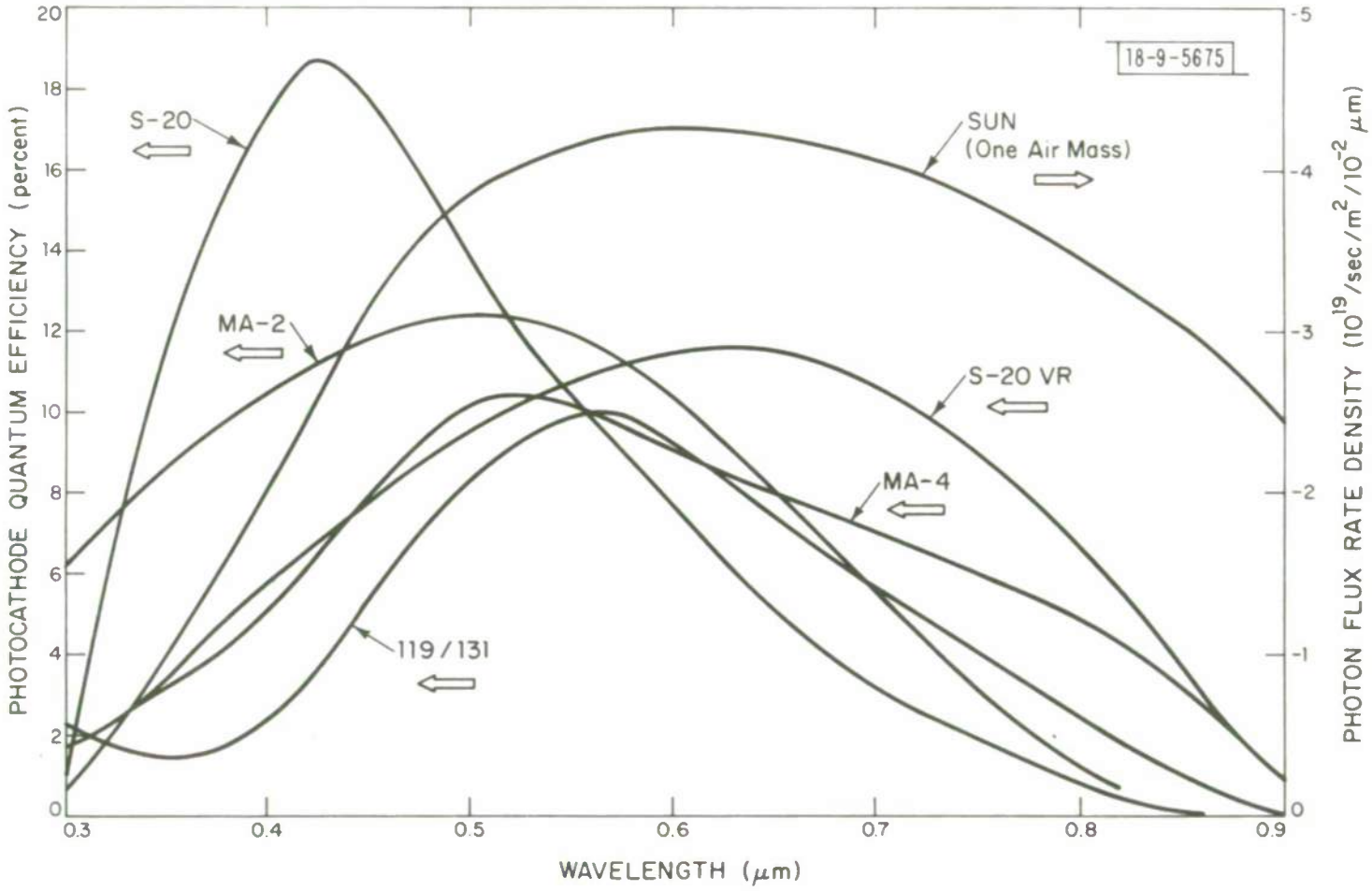

Fig.1. Quantum efficiencies of selected photosurfaces and photon flux rate density of "one-air-mass" sunlight as a function of wavelength.

relative merits of the S-20 and S-20VR surfaces will be altered. In Appendix A may be found the tabulated results for this section of this report.

TABLE I

The normalized (to S-20) result of convolving the quantum efficiency curves of the given photosurfaces with the photon flux rate density of "one-air-mass" sunlight.

Photosurface	Normalized Photoelectron Flux Rate Density	Maximum Increase in Detection Signal Magnitude
S-20	1.00	---
119/131	0.79	-0.26
MA-2	1.02	+0.02
MA-4	0.99	---
S-20VR	1.20	+0.20

Figure 2 presents the wavelength curves for P-11 and P-20 phosphors, and for S-20 and S-20VR photosurfaces. The ordinate for the phosphors is given in photons emitted per absorbed 10kV photoelectron per nm at a given wavelength. Assuming perfect coupling between the phosphor and the photo-emissive surface, the multiplication and summation of appropriate entries on the graph, for a given sandwich, directly yields a measure of the maximum current gain to be expected from the combination. In the real situation, the coupling efficienty via fiber-optic plates, is of the order of fifty percent.

The S-20 and S-20VR photosurfaces are stressed in this section for two reasons. Two of the surfaces (MA-2, and 119/131), considered earlier, clearly are not as efficient as the S-20 and S-20VR surfaces when used with phosphors of the type listed above, while the third surface, MA-4, is surpassed in per-formance is most instances. The second reason for stressing S-20 and S-20VR

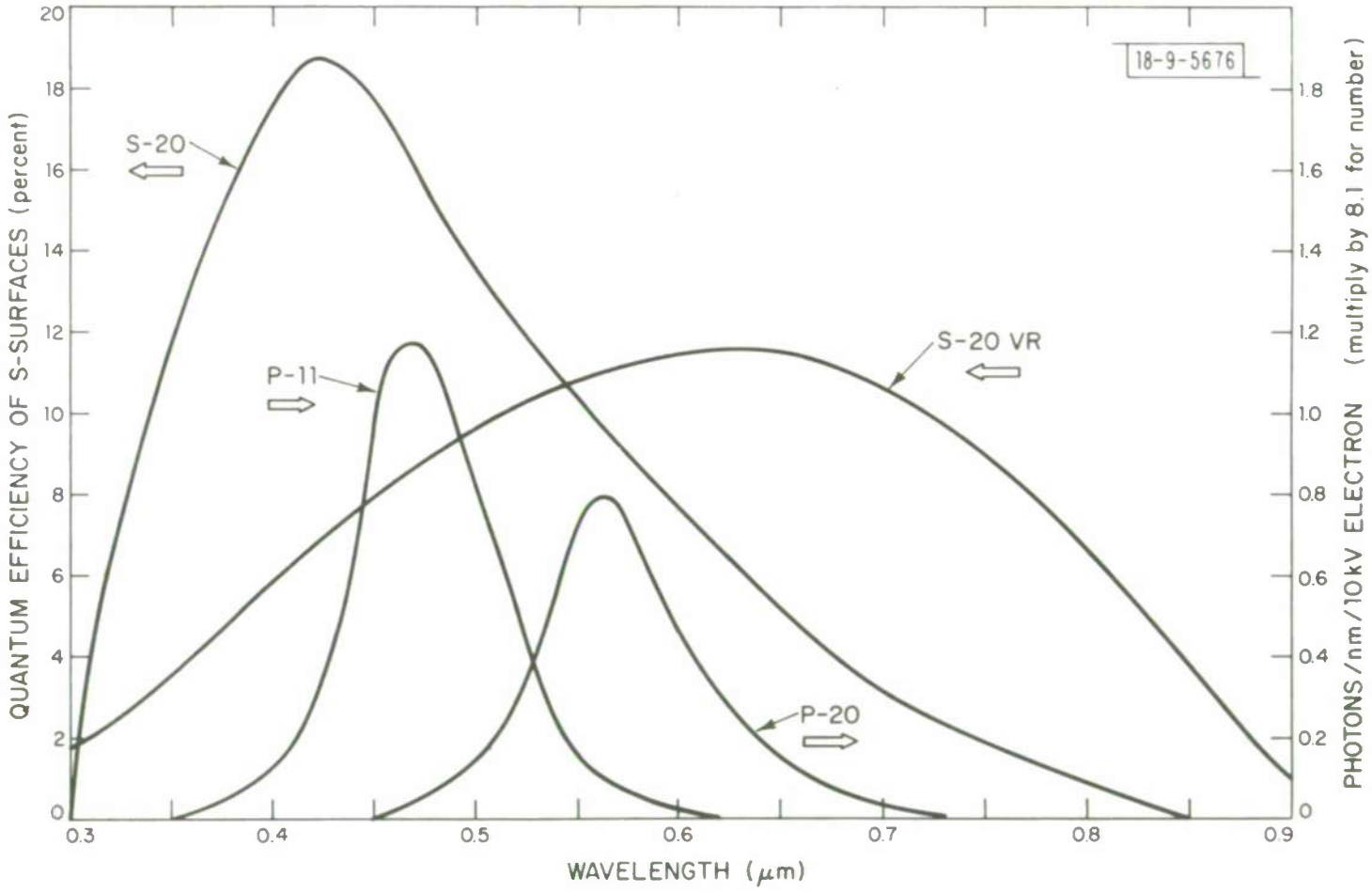

Fig.2. Quantum efficiencies of S-20 and S-20VR surfaces and responses of P-11 and P-20 surfaces as a function of wavelength.

photosurfaces is that they are more widely available than are the other photosurfaces.

Table II summarizes the current gain to be expected from the various sandwich combinations. The results have been normalized to the P-20/S-20 combination. It is clear that P-11/S-20 yields the highest possible current gain, approximately 2.3 times that of the commonly used P-20/S-20 combination. For equal current-gain requirements, the former case would require less than one-half the photoelectron accelerating potential required in the latter case. This is a significant advantage in cascaded systems in which one is dealing with tens of kilovolts of accelerating potential-difference between the first photocathode and the target-plane of the camera tube. The frequency of internal ionic events and breakdown events should be reduced drastically at the lower potential difference.

The tabulated results for this section of this report may be found in Appendix B.

TABLE II

The current-gain to be expected of various phosphor/photocathode combinations. The results have been normalized to the P-20/S-20 combination.

Phosphor	S-20	S-20VR	MA-4
P-20	1.00	1.15	1.05
P-11	2.29	1.27	1.32

RECOMMENDATIONS AND CONCLUSIONS

1. Unintensified ("Bare") Camera Tube.

Optimum performance will be achieved by the incorporation of an S-20VR photosurface in the image section of the bare camera tube, as the first photocathode. However, the realization of an S-20VR surface in an integrated camera tube may incur added costs in that the majority of the manufacturers of ebsicon-type camera tubes are "geared to" the fabrication of S-20 surfaces. That is, a number of experimental tube "starts" may be required to bring the technology of a given manufacturer to the point that satisfactory S-20VR surfaces may be fabricated with the same consistency with which S-20 surfaces are fabricated at the present time. If the added costs prove to be reasonable, this is the way to proceed. Then, for a given "sun-like" optical signal, the signal photoelectron flux rate density will be increased by twenty percent over that provided by the popular S-20 first photocathode.

2. Intensified Camera Tube.

It is clear from Table II that the "sandwich" between the external image intensifier and the ebsicon-type camera tube should consist of a P-11 phosphor and an S-20 photoemissive surface. The current gain in this instance will be approximately 2.3 times greater than that for the widely used P-20/S-20 sandwich. The significant practical advantages have already been described.

In this case, unlike the case of the bare camera tube, there is no problem in obtaining a first photosurface (now on the intensifier) of S-20VR material. Thus, the maximum increase in the signal charge at the target of the sensor for a given "sun-like" optical signal will be $1.2 \times 2.3 = 2.8$ times that to be expected for an externally intensified camera-tube sensor employing S-20 and P-20 materials, and operating at the same potential-difference levels.

From the above, it is concluded that the "no risk" approach - and one that achieves maximum performance - for the externally intensified sensor is to incorporate an S-20VR first photocathode and a P-11 anode in the intensifier, and to couple this to the S-20 second photocathode of a camera tube.

In the case of the bare tube, while an S-20VR photocathode is obviously desirable, its fabrication in an ebsicon-type camera tube may present initial difficulties. This fact, coupled with the possible wish for the interchangability of camera tubes in a given system, may well lead to the decision to specify S-20 photosurfaces for all camera tubes, whatever the application, thereby foregoing tha improvement promised by the S-20VR photosurface in the bare tube application.

ACKNOWLEDGEMENTS

Thanks are due to J. W. McLellan for performing the calculations, to D. J. Mancuso for typing the draft, and to D. M. Campo for typing the Appendices and the final manuscript.

REFERENCES

1. R. Weber, "Visual Magnitude Flux Rate Density Standards for Sunlight Incident on Photoemissive Surfaces," Technical Note 1974-20, Lincoln Laboratory, M.I.T. (6 May 1974), DDC AD-779822/6.

APPENDIX A

PHOTOELECTRON FLUX RATE DENSITIES OF SELECTED PHOTOEMISSIVE SURFACES EXPOSED TO "ONE-AIR-MASS" SUN LIGHT

Definitions of Column Headings

$\Delta\lambda$	wavelength interval, in microns.
λ	wavelength, in microns.
SUN (S)	the photon flux rate density of "one-air-mass" sunlight within $\Delta\lambda$. (10^{19} sec^{-1} $m^{-2}/10^{-2}\mu m$.)
S-20 MA-2 S20-VR MA-4 119/131	quantum efficiency of photoemissive surface, in percent.
119/131·S S-20·S MA-2·S S20-VR·S MA-4·S	convolution of each surface with S within $\Delta\lambda$. These entries are the photoelectron flux rate densities.

APPENDIX A

Δλ	λ	SUN, S	S-20	MA-2	S20-VR	MA-4	119/131
0.02	0.30	0.28	1.00	6.20	1.7	1.7	2.2
	.32	0.90	6.90	7.20	2.2	2.2	1.8
	.34	1.70	10.40	8.20	2.9	3.0	3.0
	.36	2.00	13.40	9.00	4.0	3.4	1.45
	.38	2.52	15.50	10.00	4.9	4.1	1.75
	.40	3.68	17.50	10.50	5.9	5.0	2.3
	.42	5.10	18.70	11.0	6.7	6.2	3.4
	.44	5.84	18.60	11.6	7.4	7.4	4.65
	.46	7.18	17.10	12.0	8.0	8.5	5.95
	.48	7.60	15.10	12.3	8.9	9.5	7.25
	.50	7.82	13.40	12.4	9.5	10.4	8.35
	.52	7.88	12.20	12.3	10.1	10.4	9.15
	.54	8.04	10.90	12.1	10.5	10.3	9.7
	.56	8.30	9.90	11.8	10.9	10.0	10.0
	.58	8.52	8.80	11.1	11.2	9.5	9.9
	.60	8.56	7.70	10.5	11.4	9.1	9.3
	.62	8.50	6.70	9.5	11.5	8.7	8.55
	.64	8.46	5.70	8.5	11.5	8.2	7.85
	.66	8.40	4.70	7.8	11.4	7.9	7.1
	.68	8.20	3.80	6.6	11.0	7.5	6.4
	.70	8.10	3.10	5.0	10.8	7.1	5.15
	.72	8.08	2.60	4.6	10.0	6.8	5.0
	.74	7.70	2.20	3.8	9.5	6.3	4.3
	.76	7.50	1.70	2.8	8.6	5.8	3.7
	.78	7.20	1.30	2.0	7.9	5.4	3.05
	.80	6.96	0.90	1.2	6.7	5.0	2.5
	.82	6.66	0.50		5.4	4.4	1.85
	.84	6.26	0.20		4.5	3.5	1.25
	.86	5.78	0.05		3.1	3.0	0.75
	.88	5.42			2.0	2.0	0.35
	.90	4.92			0.9	1.1	0.05
	.92	4.52					
		198.58					

APPENDIX A (Continued)

$\Delta\lambda$	λ	119/131·S	S-20·S	MA-2·S	S20-VR·S	MA-4·S
0.02	0.30	0.62	0.28	1.74	0.48	0.48
	.32	1.62	6.21	6.48	1.98	1.98
	.34	2.55	17.68	13.94	4.93	5.10
	.36	2.90	26.80	18.00	8.00	6.80
	.38	4.41	39.06	25.20	12.35	10.33
	.40	8.46	64.40	38.64	21.71	18.40
	.42	17.34	95.37	56.10	34.17	31.62
	.44	27.16	108.63	67.75	43.22	43.22
	.46	42.72	122.78	86.16	57.44	61.03
	.48	55.10	114.76	93.48	67.64	72.20
	.50	65.29	104.79	96.97	74.29	81.33
	.52	72.10	96.14	96.93	79.59	81.95
	.54	77.99	87.64	97.28	84.42	82.81
	.56	83.00	82.17	97.94	90.47	83.00
	.58	84.35	74.98	94.57	95.42	80.94
	.60	79.61	65.91	89.88	97.58	77.89
	.62	72.68	56.95	80.75	97.75	73.95
	.64	66.41	48.22	71.91	97.29	69.37
	.66	59.64	39.48	65.52	95.76	66.36
	.68	52.48	31.16	54.12	90.20	61.50
	.70	45.77	25.11	40.50	87.48	57.51
	.72	40.40	21.01	37.17	80.80	54.94
	.74	33.11	16.94	29.26	73.15	48.51
	.76	27.75	12.75	21.00	64.50	43.50
	.78	21.96	9.36	14.40	56.88	38.88
	.80	17.40	6.26	8.35	46.63	34.80
	.82	12.32	3.33		35.96	29.30
	.84	7.83	1.25		28.17	21.91
	.86	4.34	0.29		17.92	17.34
	.88	1.92			10.84	10.84
	.90	0.25			4.43	5.41
		1089.48	1379.71	1404.04	1661.45	1373.19

APPENDIX B

SANDWICH "CURRENTS" OF SELECTED COMBINATIONS
OF PHOSPHORS AND PHOTOEMISSIVE SURFACES

Definitions of Column Headings

$\Delta\lambda$	wavelength interval in microns.
λ	wavelength, in microns.
P11	phosphor responses. (Photons per nm interval per 10 k V electron. These entries have not been multiplied by 8.1 for the actual number of photons.)
P20	
S-20	quantum efficiency of each photosurface, in percent.
S20-VR	
MA-4	
P20·MA-4	entries proportional to sandwich current within $\Delta\lambda$ interval.
P11·S20	
P11·S20-VR	
P20·S20	
P20·S20VR	
P11·MA-4	

APPENDIX B

Δλ	λ	P11	P20	S20	S20VR	MA-4
0.01	0.35	0.00		12.00	4.00	3.20
	.36	0.20		13.50	4.30	3.40
	.37	0.30		14.90	4.70	3.80
	.38	0.55		16.10	5.10	4.10
	.39	0.85		17.00	5.50	4.70
	.40	1.25		17.80	5.90	5.00
	.41	1.90		18.25	6.30	5.70
	.42	2.90		18.70	6.70	6.20
	.43	4.30		18.75	7.00	6.80
	.44	6.55		18.35	7.30	7.40
	.45	9.70	0.00	18.00	8.00	7.40
	.46	11.50	0.20	17.10	8.40	8.50
	.47	11.70	0.45	16.00	8.60	9.00
	.48	11.00	0.70	15.10	8.90	9.50
	.49	9.50	1.05	14.40	8.80	9.90
	.50	8.30	1.50	13.40	9.00	10.20
	.51	6.70	2.00	12.90	9.30	10.40
	.52	5.00	3.00	12.25	9.50	10.50
	.53	3.60	4.30	11.65	9.70	10.40
	.54	2.40	5.60	11.10	9.90	10.30
	.55	1.55	7.15	10.40	10.00	10.20
	.56	1.10	7.90	9.70	10.30	10.00
	.57	0.80	7.80	9.20	10.60	9.80
	.58	0.55	6.60	8.50	10.75	9.50
	.59	0.35	5.60	8.00	10.85	9.30
	.60	0.20	4.70	7.60	11.00	9.10
	.61	0.10	3.90	6.90	11.30	8.90
	.62	0.05	3.20	6.50	11.35	8.70
	.63	0.00	2.50	6.00	11.45	8.40
	.64		2.00	5.70	11.50	8.20
	.65		1.50	5.20	11.50	8.00
	.66		1.25	4.60	11.50	7.90
	.67		0.90	4.20	11.30	7.70
	.68		0.65	3.90	11.10	7.50
	.69		0.45	3.50	10.80	7.30
	.70		0.30	3.15	10.50	7.10
	.71		0.25	2.80	10.40	6.90
	.72		0.15	2.60	10.15	6.80
	.73		0.10	2.40	9.80	6.40
	.74		0.05	2.20	9.30	6.20
	.75		0.00	2.00	9.05	6.00

APPENDIX B (Continued)

Δλ	λ	P20·MA-4	P11-S20	P11·S20VR	P20·S20	P20·S20VR	P11·MA-4
0.01	0.35		0.00	0.00			0.00
	.36		2.70	0.86			0.68
	.37		4.47	1.41			1.14
	.38		8.86	2.81			2.26
	.39		14.45	4.68			4.00
	.40		22.25	7.38			6.25
	.41		34.68	11.97			10.83
	.42		54.23	19.43			17.98
	.43		80.62	30.10			29.24
	.44		120.19	47.82			48.47
	.45	0.00	174.60	77.60	0.00	0.00	71.78
	.46	1.70	196.65	96.60	3.42	1.68	97.75
	.47	4.05	187.20	100.62	7.20	3.87	105.30
	.48	6.65	166.10	95.70	10.57	6.09	104.50
	.49	10.39	136.80	83.60	15.12	9.24	94.05
	.50	15.30	111.22	74.70	20.10	13.50	84.66
	.51	20.80	86.43	62.31	25.80	18.60	69.68
	.52	31.50	61.25	47.50	36.75	28.50	52.50
	.53	44.72	41.94	34.92	50.10	41.71	37.44
	.54	57.68	26.64	23.76	62.16	55.44	24.72
	.55	72.93	16.12	15.50	74.36	71.50	15.81
	.56	79.00	10.67	11.83	76.63	81.37	11.00
	.57	76.44	7.36	8.48	71.76	82.68	7.84
	.58	62.70	4.68	5.92	56.10	70.95	5.23
	.59	52.08	2.80	3.79	44.80	60.76	3.26
	.60	42.77	1.52	2.20	35.72	51.70	1.82
	.61	34.71	0.69	1.13	26.91	44.07	0.89
	.62	27.84	0.33	0.57	20.80	36.32	.44
	.63	21.00	0.00		15.00	28.63	0.00
	.64	16.40			11.40	23.00	
	.65	12.00			7.80	17.25	
	.66	9.88			5.75	14.38	
	.67	6.93			3.78	10.17	
	.68	4.88			2.54	7.22	
	.69	3.29			1.58	4.86	
	.70	2.13			0.95	3.15	
	.71	1.73			0.70	2.60	
	.72	1.02			0.39	1.52	
	.73	.64			0.24	0.98	
	.74	.31			0.11	0.47	
	.75						
		721.47	1575.45	873.19	688.53	792.21	909.52

REPORT DOCUMENTATION PAGE

READ INSTRUCTIONS BEFORE COMPLETING FORM

1. REPORT NUMBER: ESD-TR-77-115	2. GOVT ACCESSION NO.
3. RECIPIENT'S CATALOG NUMBER	
4. TITLE (and Subtitle): Photoemissive and Electroemissive Surfaces and Sandwiches	5. TYPE OF REPORT & PERIOD COVERED: Technical Note
6. PERFORMING ORG. REPORT NUMBER: Technical Note 1977-18	
7. AUTHOR(s): Robert Weber	8. CONTRACT OR GRANT NUMBER(s): F19628-76-C-0002
9. PERFORMING ORGANIZATION NAME AND ADDRESS: Lincoln Laboratory, M.I.T. P.O. Box 73 Lexington, MA 02173	10. PROGRAM ELEMENT, PROJECT, TASK AREA & WORK UNIT NUMBERS: Program Element No. 63428F Project No. 2128
11. CONTROLLING OFFICE NAME AND ADDRESS: Air Force Systems Command, USAF Andrews AFB Washington, DC 20331	12. REPORT DATE: 25 May 1977
	13. NUMBER OF PAGES: 20
14. MONITORING AGENCY NAME & ADDRESS (if different from Controlling Office): Electronic Systems Division Hanscom AFB Bedford, MA 01731	15. SECURITY CLASS. (of this report): Unclassified
	15a. DECLASSIFICATION DOWNGRADING SCHEDULE

16. DISTRIBUTION STATEMENT (of this Report)

Approved for public release; distribution unlimited.

17. DISTRIBUTION STATEMENT (of the abstract entered in Block 20, if different from Report)

18. SUPPLEMENTARY NOTES

None

19. KEY WORDS (Continue on reverse side if necessary and identify by block number)

photoemissive surfaces
electroemissive surfaces
optical sensor
space object detection

20. ABSTRACT (Continue on reverse side if necessary and identify by block number)

Several commercially available photoemissive surfaces (PES) and electroemissive surfaces (ES) are evaluated to find: 1. the most efficient PES in the presence of sunlight-like optical signals, and, 2. the most efficient ES/PES combination ("sandwich") for the transition between stages in an optical sensor employing, for example, an image intensifier tube coupled to an ebsicon-type camera tube. In the first case, an S-20VR PES is shown to be superior; while in the second case, a P-11/S-20 sandwich is shown to be the superior combination.